Microscopic model for the structural transition and spin gap formation in α'-NaV$_2$O$_5$

A. Bernert,[1] P. Thalmeier,[2] and P. Fulde[1]

[1] *Max-Planck-Institut für Physik komplexer Systeme, D-01187 Dresden, Germany*
[2] *Max-Planck-Institut für Chemische Physik fester Stoffe, D-01187 Dresden, Germany*

We present a microscopic model for α'-NaV$_2$O$_5$. Using an extended Hubbard model for the vanadium layers we derive an effective low-energy model consisting of pseudospin Ising chains and Heisenberg chains coupled to each other. We find a "spin-Peierls-Ising" phase transition which causes charge ordering on every second ladder and superexchange alternation on the other ladders. This transition can be identified with the first transition of the two close-by transitions observed in experiment. Due to charge ordering the effective coupling between the lattice and the superexchange is enhanced. This is demonstrated within a Slater-Koster approximation. It leads to a second instability with superexchange alternation on the charge-ordered ladders due to an alternating shift of the O sites on the rungs of that ladder. We can explain within our model the observed spin gap, the anomalous BCS ratio, and the anomalous shift of the critical temperature of the first transition in a magnetic field. To test the calculated superstructure we determine the low-energy magnon dispersion and find agreement with experiment.

I. INTRODUCTION

The layered oxide α'-NaV$_2$O$_5$ has attracted great interest since 1996, when Isobe and Ueda reported a phase transition at $T=34$ K with a spin-Peierls like spin gap formation.[1] At low temperatures the spin gap has a size of about $\Delta \approx 100$ K,[1–3] which yields a BCS ratio $2\Delta/k_B T_C \approx 6$, much higher than for other organic or inorganic spin-Peierls materials, for which it lies around the canonical BCS-value of 3.5.

Furthermore, experiments have shown that there are actually *two* transitions, which lie very close to each other.[4,5] Both are of second order. The first one at $T_{C1} \approx 34$ K is accompanied by a logarithmic peak in the specific heat[6,7] while the second at $T_{C1} - T_{C2} \approx 0.3$ K is of mean-field character evident from a jump in the specific heat. NMR measurements suggest that the first transition leads to charge ordering while the second one opens a spin gap.[5]

Measurements of the critical exponents yield $\beta_\delta \approx 0.15 \cdots 0.2$ for the critical exponent of the lattice distortion δ and $\beta_\Delta \approx 0.34$ for the critical exponent of the spin gap Δ.[8–11] From these values the existence of two transition can also be inferred indirectly. Close to the critical point the spin gap Δ due to a lattice distortion δ is expected to obey $\Delta \propto \delta^{3/4}$,[12] corresponding to $\beta_\Delta = 3/4 \beta_\delta$. This relation is not fulfilled in α'-NaV$_2$O$_5$, indicating the existence of two separate transitions.

For $T > T_{C1}$ α'-NaV$_2$O$_5$ has equivalent V sites[13–15] implying valence 4.5+. For $T < T_{C2}$ early ^{51}V-NMR measurements show only two inequivalent sites[16] while x-ray structure determination reports three inequivalent sites[17–19] as do recent ^{51}V-NMR measurements.[20] Recently, new experiments found two inequivalent V sites per layer by use of anomalous x-ray scattering[21] and high resolution x-ray data,[22] while another x-ray structure determination found four inequivalent V sites[23] per layer, two of which have similar charge.

An interesting experimental observation is the magnetic field dependence of T_{C1}. It is only about 25% of the value expected for a spin-Peierls transition[4,24,25] but on the other hand, it is much higher than what would be generally expected for a structural transition.[26]

In this article we explain a number of these above mentioned features by an analysis of a microscopic model. We find that the phase transition at T_{C1} can be regarded as a combination of charge ordering on every second ladder and superexchange alternation on the other ladders, a "spin-Peierls-Ising" transition. This also explains the anomalous shift of T_{C1} in a magnetic field. The phase transition at T_{C2} can be regarded as a spin-Peierls transition on the charge-ordered ladders. It is driven by the charge ordering. The lattice distortion accompanying the charge ordering increases the coupling constant of a lattice mode invoking superexchange alternation on the charge-ordered ladders. With increasing charge ordering for decreasing temperatures the coupling constant increases until the second phase transition takes place at T_{C2}. This second phase transition opens a spin gap in agreement with experimental observations. Charge ordering is not yet complete at T_{C2}. The coupling constant therefore continues to increase and due to this the low-temperature spin gap is larger than what would be expected from T_{C2}, i.e., the BCS ratio is enhanced.

We test our low-temperature structure against x-ray structure determination and find it to agree within experimental resolution. Furthermore we calculate the low-energy magnon dispersion and find it to agree nicely with experimental results from inelastic neutron scattering.[2,3]

In the following we give an outline of the way our article is organized and the rationale behind choosing the models and the contributions that have to be present in the Hamiltonian in order to describe the observations mentioned before. In the first part of Sec. II we start from a model that involves only electronic degrees of freedom. It is of the extended Hubbard type including intersite Coulomb repulsion. This is a necessary ingredient for a possible charge ordering transition. Because the on-site Coulomb interaction U is

much bigger than the intersite interactions and the hopping energies one may project to an effective low energy model involving only singly occupied V-V rungs that are represented by an pseudospin $\frac{1}{2}$.[27–29] This reduced but still purely electronic model is of the Ising type in a "transverse field" where the latter is given by the intra-rung hopping. If this is sufficiently small the model has a quantum critical point where a zig-zag charge ordered ground state of the single ladder sets in. However, due to the geometric frustration of the Trellis lattice a 2D charge ordered state does not exist at finite temperature. To describe the α'-NaV$_2$O$_5$ phase transitions it is therefore necessary to include spins and lattice distortions as additional degrees of freedom.

This is done in the second part of Sec. II. For a charge ordering at finite temperature the geometric frustration needs to be removed. For this purpose spin and lattice degrees of freedom have to be involved such that the spin-Peierls Ising transition mentioned above generates inequivalent ladders with charge order appearing only on every second ladder. The derivation and physical background of this extended Ising spin-Peierls Hamiltonian is given at the end of Sec. II.

In Sec. III A we analyze this Hamiltonian by using Cross-Fisher theory for the individual ladders and an RPA approach for the coupled 2D lattice. Sec. III B describes in quantitative detail the spin-Peierls Ising phase transition in the 2D Trellis lattice at T_{C1} which creates alternating sets of charge ordered (A) and exchange dimerized (B) ladders. In Sec. III C we show how the evolving charge order on one type of ladder (A) below T_{C2} increases the coupling to an exchange dimerization mode on the same ladder. This leads to a second transition at T_{C2} immediately below T_{C1} which is responsible for the opening of the spin gap observed in the susceptibility.

In Sec. IV we compare the calculated low temperature structure with experiment. With regards to the x-ray structure determination we argue that within experimental resolution theory and experiment agree. Using this structure we calculate the dispersion of gapped spin excitations parallel and perpendicular to the chain direction. The latter contains information on the charge ordered structure and allows one to extract various experimental exchange constants. We find that an additional splitting of spin excitation modes at zone boundary points is very well explained within the inequivalent ladder model proposed. Finally Sec. V gives the summary and conclusions.

II. DERIVATION OF THE MODEL HAMILTONIAN

To construct a model Hamiltonian we note that according to LDA+U calculations[30] the orbitals around the Fermi level are mostly of vanadium d_{xy} character. They are separated both from the lower lying oxygen p orbitals as well as from the remaining vanadium d orbitals and the sodium $3s$ orbital which lie energetically higher. This means that we have to consider only the quarter filled d_{xy} orbitals. For a discussion of charge ordering we restrict ourselves to a 2D model neglecting hopping matrix elements and Coulomb interactions between the vanadium layers. The former have been shown to be negligible both by LDA+U (Ref. 30) and Slater-Koster
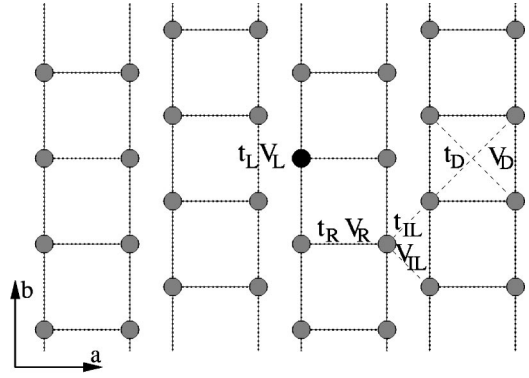

FIG. 1. Hopping matrix elements and Coulomb interactions in the V layers.

type calculations.[19] The Coulomb interactions are expected to be small due to the large distance between the V sites of neighboring layers. They are also screened by intermediate O ions. However, this interlayer interaction should play a role for the explanation of the devil's staircase observed in the p-T-phase diagram.[31] Therefore our initial Hamiltonian represents an extended one-band Hubbard model at quarter filling, taking on-site and intersite Coulomb interactions into account:

$$
\begin{aligned}
H = & \sum_{\langle i,j\rangle_R} t_R(a_{i\sigma}^\dagger a_{j\sigma}+\text{H.c.}) + \sum_{\langle i,j\rangle_L} t_L(a_{i\sigma}^\dagger a_{j\sigma}+\text{H.c.}) \\
& + \sum_{\langle i,j\rangle_{IL}} t_{IL}(a_{i\sigma}^\dagger a_{j\sigma}+\text{H.c.}) + \sum_{\langle i,j\rangle_D} t_D(a_{i\sigma}^\dagger a_{j\sigma}+\text{H.c.}) \\
& + \sum_{\langle i,j\rangle_R} V_R n_i n_j + \sum_{\langle i,j\rangle_L} V_L n_i n_j \\
& + \sum_{\langle i,j\rangle_{IL}} V_{IL} n_i n_j + \sum_i U n_{i\uparrow} n_{i\downarrow}. \quad (1)
\end{aligned}
$$

Here $\langle,\rangle_{IL}$ denotes pairs of nearest-neighbor vanadium d_{xy} orbitals while $\langle,\rangle_R$ and $\langle,\rangle_L$ denote pairs of next-nearest-neighbor vanadium d_{xy} orbitals along the rung (R) or the leg (L). The first four terms describe the effective hopping of the d electrons between V sites i and j. This hopping can take place both via oxygen orbitals and sodium orbitals. The last four terms describe the intersite and on-site Coulomb repulsion. These terms connect sites as shown in Fig. 1.

At $T>T_{C1}$ the system is at quarter filling and the V sites are all equivalent.[13] Therefore there is an average of one electron per rung. The on-site[15,32] and the intersite Coulomb repulsion create a charge transfer gap, causing α'-NaV$_2$O$_5$ to be an insulator. Therefore hopping between rungs takes place only virtually. This enables us to use an effective Hamilton operator $\tilde{H}_{PP}$ which acts on the Hilbert subspace $\mathcal{P}$ of all states with one electron on each rung. Let $\mathcal{Q}$ be the Hilbert subspace complementary to $\mathcal{P}$ and P be the projector onto $\mathcal{P}$ and Q the projector onto $\mathcal{Q}$. An eigenstate $|\psi_{PP}^{(0)}\rangle$ of $\tilde{H}_{PP}$ satisfies

$$\tilde{H}_{PP}|\psi_{PP}^{(0)}\rangle=[PHP-PHQ(QHQ-E_0)^{-1}QHP]|\psi_{PP}^{(0)}\rangle$$

$$=E_0|\psi_{PP}^{(0)}\rangle. \qquad (2)$$

To calculate $\tilde{H}_{PP}$ we need to know the energies E_0 which can be either determined self-consistently or, as for a Schrieffer-Wolff transformation, set equal to the eigenenergy E_0^{PP} of PHP. In the following we are interested in $\tilde{H}_{PP}$ only to order $O(t^2/E)$, i.e., to second order in the hopping. In this case we can neglect the hopping terms in $(QHQ-E_0)$, since both PHQ and QHP scale with t.

Within the subspace $\mathcal{P}$ we use the operators $a_{i\alpha\sigma}^{\dagger}$, $a_{i\alpha\sigma}$ for the electrons in the atomic orbitals. Here i denotes the rung, the pseudospin variable $\alpha=\pm\frac{1}{2}$ describes whether the electron occupies the left $(-\frac{1}{2})$ or right $(+\frac{1}{2})$ V site of a rung and σ denotes the z component of the spin. Using these operators we define the conditional creation operators

$$\hat{a}_{i\alpha\sigma}^{\dagger}=(1-n_{i\bar{\alpha}\uparrow})(1-n_{i\bar{\alpha}\downarrow})(1-n_{i\alpha\bar{\sigma}})a_{i\alpha\sigma}^{\dagger}$$

similar to the operators used in the t-J model.[33] We then obtain for $\tilde{H}_{PP}$

$$\tilde{H}_{PP}=H_S+\sum_i 2\hat{\tilde{t}}_R^i T_i^x+\sum_{\langle i,j\rangle_{IL}} \hat{K}_{IL}^{ij} T_i^z T_j^z$$

$$+\sum_{\langle i,j\rangle_L} (\hat{K}_{Lz}^{ij} T_i^z T_j^z+\hat{K}_{Lx}^{ij} T_i^x T_j^x+\hat{K}_{Ly}^{ij} T_i^y T_j^y), \qquad (3)$$

where $\hat{K}$, H_S, and $\hat{\tilde{t}}_R$ contain spin operator products. It turns out to be useful to work with spin and pseudospin operators

$$\vec{S}_i=\frac{1}{2}\sum_{\sigma_1,\sigma_2,\alpha} \hat{a}_{i\alpha\sigma_1}^{\dagger} \vec{\sigma}_{\sigma_1\sigma_2} \hat{a}_{i\alpha\sigma_2},$$

$$\vec{T}_i=\frac{1}{2}\sum_{\sigma,\alpha_1,\alpha_2} \hat{a}_{i\alpha_1\sigma}^{\dagger} \vec{\sigma}_{\alpha_1\alpha_2} \hat{a}_{i\alpha_2\sigma}.$$

In Eq. (3) $\vec{S}_i$ denotes the spin of the electron on the ith rung and the z component of $\vec{T}_i$ corresponds to α, so the pseudospin $\vec{T}_i$ describes the hopping of the electron between the two V sites of a rung. The first term of Eq. (3) describes the effective interaction between spins on neighboring rungs. The second term describes the hopping of the charge between the right and the left vanadium site of a rung. This hopping also depends on spin-spin interactions. The third term and $\hat{K}_{Lz}$ describe the Coulomb interaction between charges on neighboring rungs. These interactions are modified due to the interrung hopping; thus they contain spin-spin interactions. $\hat{K}_{Lx}$ and $\hat{K}_{Ly}$ also result from the interrung-hopping which has been projected out in the transfer from Eq. (1) to Eq. (3). Within second order perturbation theory these terms have the following form:

$$H_S=\sum_{\langle i,j\rangle_L} \left(\frac{2t_D^2}{U+\Delta_D^U-E_0^{PP}}+\frac{2t_L^2}{U+\Delta_L^U-E_0^{PP}}\right)\left(\vec{S}_i\vec{S}_j-\frac{1}{4}\right),$$

$$\hat{\tilde{t}}_R^i=t_R+\sum_{\langle i,j\rangle_L} t_L t_D \left(\frac{4\vec{S}_i\vec{S}_j-1}{2(U+\Delta_{LD}^U-E_0^{PP})}\right.$$

$$\left.+\frac{4\vec{S}_i\vec{S}_j-1}{2(V_R+\Delta_{LD}^V-E_0^{PP})}\right),$$

$$\hat{K}_{IL}^{ij}=-V_{IL}-\frac{t_{IL}^2(4\vec{S}_i\vec{S}_j-1)}{U+\Delta_{IL}^U-E_0^{PP}}-\frac{2t_{IL}^2}{V_R+\Delta_{IL}^V-E_0^{PP}},$$

$$\hat{K}_{Lz}^{ij}=2V_L+\frac{2t_L^2(4\vec{S}_i\vec{S}_j-1)}{U+\Delta_L^U-E_0^{PP}}-\frac{2t_D^2(4\vec{S}_i\vec{S}_j-1)}{U+\Delta_D^U-E_0^{PP}}$$

$$+\frac{4t_L^2}{V_R+\Delta_L^V-E_0^{PP}}-\frac{4t_D^2}{V_R+\Delta_D^V-E_0^{PP}},$$

$$\hat{K}_{Lx}^{ij}=\frac{2t_L^2(4\vec{S}_i\vec{S}_j+1)}{V_R+\Delta_L^V-E_0^{PP}}+\frac{2t_D^2(4\vec{S}_i\vec{S}_j+1)}{V_R+\Delta_D^V-E_0^{PP}},$$

$$\hat{K}_{Ly}^{ij}=\frac{2t_L^2(4\vec{S}_i\vec{S}_j+1)}{V_R+\Delta_L^V-E_0^{PP}}-\frac{2t_D^2(4\vec{S}_i\vec{S}_j+1)}{V_R+\Delta_D^V-E_0^{PP}}. \qquad (4)$$

Here Δ^V and Δ^U are additional energy differences due to the local change of occupation numbers with hoppings. $\hat{K}_{Lz}$ and $\hat{K}_{IL}$ describe the most important interactions between electrons on neighboring V sites. They drive the system to local "zig-zag" type ordering or local "in-line" type ordering of the V $3d$ electrons. Assuming that we have locally complete "zig-zag" short-range "ordering" within a ladder and no correlations between ladders the Δ^V, Δ^U are given by

$$\Delta_L^V=V_L, \quad \Delta_D^V=0, \quad \Delta_{IL}^V=2V_L,$$

$$\Delta_{LD}^V=0, \quad \Delta_L^U=-V_L, \quad \Delta_D^U=0,$$

$$\Delta_{IL}^U=-V_{IL}, \quad \Delta_{LD}^U=-V_L. \qquad (5)$$

Assuming that we have local "in-line ordering," they are equal to

$$\Delta_L^V=V_{IL}-V_L, \quad \Delta_D^V=2V_{IL}-2V_L,$$

$$\Delta_{IL}^V=V_{IL}-2V_L, \quad \Delta_{LD}^V=0,$$

$$\Delta_L^U=-2V_{IL}, \quad \Delta_D^U=V_{IL},$$

$$\Delta_{IL}^U=-V_{IL}, \quad \Delta_{LD}^U=0. \qquad (6)$$

We now make a mean-field approximation for the spin operator products contained in $\hat{K}$ and $\hat{\tilde{t}}_R$. With this we obtain an effective pseudospin model for the charge degrees of freedom. $K=\langle\hat{K}\rangle$ and $\tilde{t}_R=\langle\hat{\tilde{t}}_R\rangle$ become effective pseudospin coupling constants. This approximation should be acceptable since the corrections of the pseudospin part due to spin-spin interactions are moderate.

With this approximation $\tilde{H}_{PP}$ becomes the Hamiltonian for a strongly anisotropic pseudospin Heisenberg model in an "external field" $2\tilde{t}_R$. We calculate the effective coefficients $\tilde{t}_R$, K_L, K_{IL} assuming that $\langle \vec{S}_i \vec{S}_{i+1} \rangle = -\frac{3}{4}$ along the ladders and $\langle \vec{S}_i \vec{S}_j \rangle = \frac{1}{4}$ between ladders. This assumption is based on the LDA+U results for the sign of the intra-ladder and interladder exchange constants.[30] We use Δ^V, Δ^U from Eq. (5) for the case of local "zig-zag" "ordering" and set E_0^{PP} to be the ground-state energy for PHP. E_0^{PP} is then given by the expression for the ground-state energy of the Ising chain in a transverse field[34] represented by t_R:

$$E_0 = 2(2t_R)\frac{|1-\lambda_0|}{\pi}E\left(2\sqrt{\frac{-\lambda_0}{(\lambda_0-1)^2}}\right) \quad (7)$$

with $\lambda_0 = V_L/2t_R$ and E the complete elliptic integral of second kind. From the energies calculated in Ref. 30 by LDA+U for different configurations one obtains

$$2V_L - V_{IL} = 0.027 \text{ eV}. \quad (8)$$

To find V_R we assume that it can be obtained from V_L by scaling by d^3 with the different distances d of the V sites. Using the values for the parameters from Ref. 19, i.e., $t_R = -0.172$ eV, $t_L = -0.049$ eV, $t_D = -0.062$ eV, $t_{IL} = 0.110$ eV, $V_L = 2t_R$, and $U = 4$ eV, we find

$$\tilde{t}_R = -0.190 \text{ eV},$$

$$K_{IL} = -0.677 \text{ eV},$$

$$K_{Lz} = 0.679 \text{ eV},$$

$$K_{Lx} = -0.027 \text{ eV},$$

$$K_{Ly} = 0.011 \text{ eV}. \quad (9)$$

K_{Lx} and K_{Ly} are smaller than the other parameters by more than one order of magnitude and will therefore be neglected. Thus our model consists of Ising interactions K_{Lz}, K_{IL} and a "transverse field" $2\tilde{t}_R$

$$H_1 = \sum_{\langle i,j \rangle_L} K_{Lz} T_i^z T_j^z + \sum_{\langle i,j \rangle_{IL}} K_{IL} T_i^z T_j^z + \sum_i 2\tilde{t}_R T_i^x. \quad (10)$$

The resulting geometry is triangular, as can be seen in Fig. 2(a). Note that the first term is antiferromagnetic and the second term is ferromagnetic, resulting in geometrical frustration for the first two terms of Eq. (10).

We first consider the case $\tilde{t}_R = 0$. For this case the the relation between the absolute sizes of K_{Lz} and K_{IL} determines the behavior of the system.[35] If $|K_{Lz}| < |K_{IL}|$ the system undergoes a phase transition at some finite temperature into a low-temperature "ferromagnetic" state of the pseudospins with 2D-long range order. This state corresponds to an "in-line" ordering of the electrons, i.e., chains of V^{4+} and V^{5+} alternate along the a direction.

If $|K_{Lz}| > |K_{IL}|$ the system remains disordered at any finite temperature. At $T=0$ it enters an antiferromagnetic state of
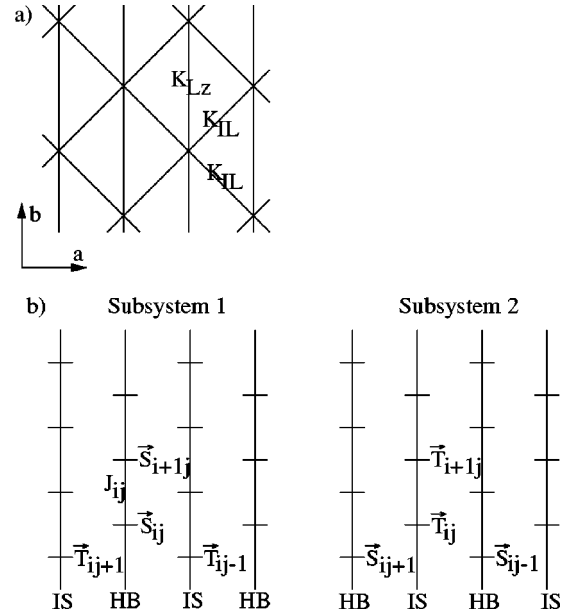

FIG. 2. (a) Lattice geometry if one introduces $\vec{S}_{ij}$ and $\vec{T}_{ij}$ operators and represents each rung by a point. (b) The two subsystems of the model described by Eq. (11) consisting of Ising (IS) pseudospin and Heisenberg (HB) spin chains.

the pseudospins with 1D order along the b direction and no correlation between neighboring ladders. This corresponds to a "zig-zag" ordering of V^{4+} and V^{5+} along the ladders. Thus the system is effectively one dimensional, although there are correlations between next-nearest-neighbor ladders.[36]

In α'-NaV$_2$O$_5$, we have $|K_{Lz}| > |K_{IL}|$. Therefore there is no phase transition at finite temperatures within the model described by Eq. (10), provided that $\tilde{t}_R = 0$ as assumed here. This is consistent with our choice of Δ^V, Δ^U. This qualitative result remains true for other choices for the hopping integrals resulting in different K_{Lz}, K_{IL}, e.g., those obtained from LDA in Ref. 30. For $\tilde{t}_R = 0$ the system is therefore close to a quantum critical point with a transition from 1D ordering in the b direction to 2D long-range order.[37]

Next we consider the case $\tilde{t}_R \neq 0$. We note that the total Hamiltonian H_1 does not imply a phase transition into an ordered state at any finite temperature. This is due to the fact that the first two terms of H_1 do not lead to a phase transition as argued above and that the nonzero transverse field suppresses ordering even more. This result remains qualitatively true if we include the K_{Lx} and K_{Ly} terms from Eq. (9) which also suppress ordering. It also remains true if we include a small interlayer Ising-like interaction. This demonstrates that the phase transitions observed in α'-NaV$_2$O$_5$ cannot be of a purely Coulombic origin: to understand what happens in this material at low temperatures we have to include at least the spin degrees of freedom beyond the mean-field approximation used above. Furthermore, we know from Raman spectroscopy that there is a strong coupling between the charge distribution on the V sites and the distortion of the system.[38] A change in the position of a V sites implies a change in the positions of the O site on the leg of the neighboring ladder.

The displacement of the O ions can in turn affect the effective superexchange interaction as observed from experimental data in Ref. 19.

Therefore we generalize the Hamiltonian from Eq. (3), such that it contains lattice degrees of freedom. Such a Hamiltonian has the following form:

$$H_{ISSP} = \sum_{i,j} \widetilde{K}_{Lz}^{ij} T_{ij}^z T_{i+1j}^z + \sum_{i,j} 2\widetilde{t}_R T_{ij}^x + \sum_{i,j} J_{ij} \vec{S}_{ij} \vec{S}_{i+1j}$$

$$+ g_{Is} \sum_{ij} T_{ij}^z \vec{e}_0 \vec{u}_{ij} + \sum_{q,j} \omega_{qj}^{VO} b_{VO,qj}^\dagger b_{VO,qj}$$

$$+ \sum_{q,j} \omega_{qj}^{Na} b_{Na,qj}^\dagger b_{Na,qj} + \sum_{q,j} \omega_{qj}^{O_R} b_{O_R,qj}^\dagger b_{O_R,qj}.$$

$$(11)$$

Here i numbers the rungs on a ladder, i.e., it denotes the (pseudo)spin on a chain, j denotes the ladder/chain in the lattice, and $\vec{e}_0$ is a unit vector. We have introduced phonon operators $b_{qj}^\dagger$, b_{qj} for the displacement of neighboring V and O ions (VO) and for the displacement of Na or rung O ions (O_R). $\vec{u}$ and J_{ij} are given by

$$J_{ij} = \left(1 + \vec{u}_{i+\frac{1}{2},j}^{VO} \vec{\nabla}_{i+\frac{1}{2},j}^{VO} + \vec{u}_{i+\frac{1}{2},j}^{Na} \vec{\nabla}_{i+\frac{1}{2},j}^{Na} + \vec{u}_{i+\frac{1}{2},j}^{O_R} \vec{\nabla}_{i+\frac{1}{2},j}^{O_R} \right)$$

$$\times J(T_{ij}^z, T_{i+1j}^z),$$

$$J(T_{ij}^z, T_{i+1j}^z) = J_0^{ij} [1 + f(T_{ij}^z, T_{i+1j}^z)],$$

$$\vec{u}_{ij} = \sum_{\lambda q} \frac{1}{(mN)^{1/2}} \exp(i\vec{q}\vec{R}_{ij}) Q_j(\lambda \vec{q}),$$

$$Q_j(\lambda \vec{q}) = b_{qj}^\dagger + b_{qj}. \qquad (12)$$

H_{ISSP} essentially describes a spin-Peierls model with additional coupling to a one-dimensional Ising chain in a transverse field. The first two terms describe the Ising model in a transverse field, the third term describes Heisenberg chains where the interaction can be changed by lattice distortion or charge fluctuations. The fourth term in H_{ISSP} gives the coupling between a lattice distortion and an effective field which leads to charge ordering. The last three terms denote the phonon dispersions of the lattice modes included in this model. The model has to take into account the following observations.

At $T=0$ K there is no correlation between pseudospins of neighboring ladders for the pure Ising interaction case. Regarding the Coulomb interactions we may therefore treat the ladders as independent, setting $K_{IL}=0$. The pseudospin part of the Hamiltonian (3) for each ladder is then described by a one-dimensional Ising model in a transverse field yielding the first two terms of H_{ISSP}. The property that the Hamiltonian (10) describes a model close to a quantum critical point has to be included in H_{ISSP}. Therefore we have to use an effective value for K_{Lz} which is close to the value needed for quantum critical behavior of the pseudospin Ising
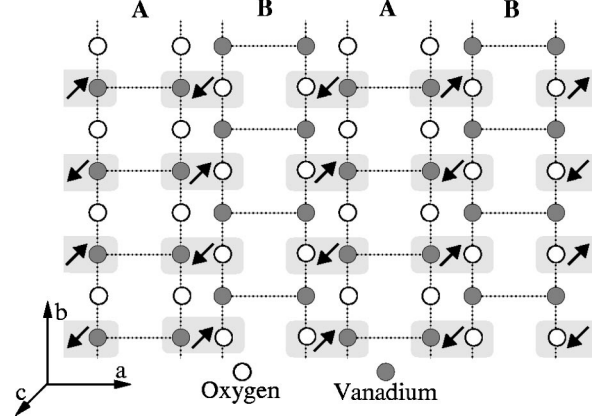

FIG. 3. The q_0 mode is shown, for which the V ion on one leg and O ion on neighboring leg move together in the c direction as shown by arrows. This causes charge ordering on A ladders due to a staggered change of the V on-site energies and superexchange alternation on B ladders due to O ion motion. In experiment (Ref. 19) shifts in the a direction are also observed which are not shown here.

chains. This effective value $\widetilde{K}_{Lz}$ is not necessarily identical to the "true" value of this Coulombic coupling in the material.

The spin part of the system behaves similar to a one-dimensional system at high temperatures,[1] i.e., we can use a one-dimensional Heisenberg model for each ladder to describe it. These terms are contained in the third term of H_{ISSP}. The magnon dispersion at low temperatures in the a direction is much smaller than in the b direction,[2,3] even though interladder spin-spin coupling has a significant value.[30] Close to the disordered phase, however, interladder coupling is reduced due to frustration: as far as interladder spin-spin coupling is concerned the system consists of triangles with one large antiferromagnetic and two smaller ferromagnetic interactions.

On each ladder spin and pseudospin degrees of freedom are coupled. This coupling is incorporated into the effective pseudospin coupling K_{Lz} and the effective coupling constant J_{ij} for the superexchange along the ladder.

A shift of V and neighboring O ions is assumed to cause an effective staggered field in the z direction for the pseudospins on one leg of a ladder described by the fourth term of H_{ISSP}. Such a shift also causes a change in the superexchange for the neighboring leg of the neighboring ladder (see Fig. 3) which has to be incorporated into the effective coupling constant J_{ij}.

As has been argued in Ref. 19, a shift of the Na ions in the c direction alternating along the ladder direction will cause an alternation in the superexchange along the ladder. The same effect is obtained by an alternating shift of O ions on a rung in the b direction. Such terms are included in J_{ij} and their significance will be examined in Sec. III C.

The last three terms of H_{ISSP} describe the energies of the important lattice modes. The spin-Peierls coupling contained in the expression for J_{ij} in Eq. (12) is slightly different from the normal form since it is the shift of the intermediate O ions or Na ions instead of the V ions, which causes the superexchange dimerization. For parameters we will use
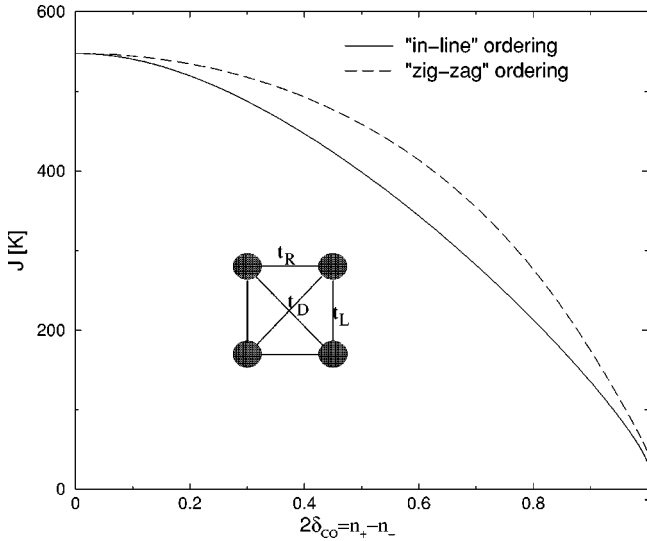
FIG. 4. Dependence of superexchange J on charge ordering. Results from cluster calculation for two rungs of the same ladder with parameters $t_R = 0.172$ eV, $t_L = 0.049$ eV, $t_D = 0.062$ eV, $V_L = 0.344$ eV, $V_R = 0.398$ eV, $U = 4$ eV and superexchange defined as the singlet-triplet gap.[19] "Zig-zag" charge ordering or "in-line" charge ordering was induced by changing the on-site energies with $\epsilon_1 = \epsilon_3 = -\epsilon_2 = -\epsilon_4$ for "in-line" ordering and $\epsilon_1 = -\epsilon_2 = -\epsilon_3 = \epsilon_4$ for "zig-zag" ordering. The inset shows geometry of cluster. The difference in the behavior of the superexchange between the two ordering patterns comes from the fact that $t_L \neq t_D$ and $V_L \neq V_D = 0$.

$\tilde{t}_R = -0.190$ eV and $J_0 = 0.045$ eV for the case without charge ordering and no distortion.

The effective superexchange along a ladder J_{ij} defined in Eq. (12) consists of three parts: J_0^{ij} denotes the original superexchange for the ladder without charge ordering or distortions. The second part, $J_0^{ij} f(T_{ij}^z, T_{i+1j}^z)$ describes the influence of the charge ordering on the superexchange. From numerical calculations we know that homogenous charge ordering on a ladder j causes a drop of the effective superexchange which is quadratic in $\langle T_j^z \rangle$, as can be seen in Fig. 4. The parabolic form of the curve can be understood from noting that the spectral weight of pair states with two particles on the same rung or the same leg decreases with $1 - (1 + \delta_{CO})(1 - \delta_{CO}) = \delta_{CO}^2$. Analytic calculations show a similar behavior.[39] Therefore $J_0^{ij} f(T_{ij}^z, T_{i+1j}^z)$ is approximately proportional to $(T_j^z)^2$ and the square of the distortion accompanying the charge ordering. If we use the experimental value for the phonon frequencies this effect is already contained in the high-temperature values of the phonon dispersion ω_{qj} and the term $J_0^{ij} f(T_{ij}^z, T_{i+1j}^z)$ is omitted, essentially making a mean-field approximation with regard to the spin operator products for this expression.

Finally, there is the essential contribution

$$\left(1 + \vec{u}_{i+\frac{1}{2},j}^{VO} \cdot \vec{\nabla}_{i+\frac{1}{2},j}^{VO} + \vec{u}_{i+\frac{1}{2},j}^{Na} \cdot \vec{\nabla}_{i+\frac{1}{2},j}^{Na} + \vec{u}_{i+\frac{1}{2},j}^{O_R} \cdot \vec{\nabla}_{i+\frac{1}{2},j}^{O_R}\right)$$
$$\times J_0^{ij}[1 + f(T_{ij}^z, T_{i+1j}^z)]$$

to the superexchange. It describes the coupling between distortion, superexchange dimerization, and charge ordering. Here we use a mean-field approximation for the pseudospin operator products. The term causes a competition between the spin-Peierls order parameter and charge order parameter on a ladder. $\tilde{K}_{Lz}$ will be fitted to properly describe the system. As argued above, we must use $\tilde{K}_{Lz}$ instead of K_{Lz} in Eq. (11).

In this section we have shown that the charge ordering mechanism may be described by an effective Ising type low energy Hamiltonian where the d electrons in singly occupied V-V rungs are described by an pseudospin. However due to the geometric frustration of the 2D Trellis lattice a charge ordering at finite temperature required the extension of the Hamiltonian to include spin and lattice degrees of freedom. The latter may lift the frustration due to a distortion of the lattice and thus facilitate a combined charge ordering and dimerization leading to inequivalent ladders A, B as shown in the next section.

III. PHASE TRANSITIONS

Now we analyze the Hamiltonian given by Eq. (11). We have two types of instabilities to consider based on the third and fourth term. The first type results from the fourth term of Eq. (11) which describes a coupling between local distortions and charge ordering. By distortion the system reduces the interaction energy. Due to elastic coupling this is also accompanied by an alternating exchange coupling on neighboring ladders. The second type results from the third term in Eq. (11) which includes a coupling between lattice and spin degrees fo freedom leading to an instability of a spin-Peierls type.

In the following subsection we separate the system into two sublattices and first treat each subsystem on its own. Using RPA we analyze in Sec. III B the first type of instability accompanied by charge ordering and superexchange alternation. We fit the free parameters g_{Is} and $\tilde{K}_{Lz}$ as to obtain the proper value of T_{C1} and the shift of T_{C1} in a magnetic field. By analyzing the ground-state energy of different ordered states we find that at low temperatures half the ladders are charge ordered and on the remaining half there is superexchange alternation.

In Sec. III C we examine the influence of charge ordering on the second type of instability. The distortions of the charge-ordered ladders change the coupling $\vec{u}_{i+\frac{1}{2},j}^{O_R} \cdot \vec{\nabla}_{i+\frac{1}{2},j}^{Q_R} J_0^{ij}$ and therefore the spin-lattice interaction. It will be shown that this interaction increases and results in a second phase transition. As shown below, this explains the anomalous BCS ratio.

A. Separation of the subsystems

The Hamiltonian (11) describes a model consisting of two subsystems 1 and 2 shown in Fig. 2(b). Both subsystems contain Ising pseudospin chains alternating with Heisenberg spin chains. The Ising pseudospin chains describe the charge distribution on a ladder, and the Heisenberg spin chains de-

scribe the spin on a neighboring ladder. The degrees of freedom on each rung (ij) are characterized by a pseudospin $\vec{T}_{ij}$ on rung (ij) which is contained in one subsystem and a spin $\vec{S}_{ij}$ contained in the other subsystem. The two subsystems 1 and 2 describe the complete spin-charge dynamics of the Hamiltonian (11).

Neighboring chains of the same subsystem are coupled by the lattice dynamics. A change of the superexchange along a spin chain is obtained, e.g., by a displacement of an O ion on a leg. Via the elastic coupling this causes a displacement of the neighboring V site (see Fig. 3). Such a local distortion changes the chemical environment and therefore the on-site energy of the vanadium d_{xy} orbital. This change in energy corresponds to a longitudinal field for the pseudospin of that rung. We assume that this field h_T^z is proportional to the displacement d_V of the V site of that rung and write

$$h_T^z = 2g_{Is}d_V. \qquad (13)$$

The two subsystems are coupled due to the dependence of the coupling J_{ij} on the charge distributions $\langle T_{ij}^z \rangle$ and $\langle T_{i+1j}^z \rangle$. J_{ij} describes the coupling of spins $\vec{S}_{ij}$ and $\vec{S}_{i+1j}$ in one subsystem and this term is contained in one subsystem, while $\langle T_{ij}^z \rangle$ and $\langle T_{i+1j}^z \rangle$ are operators used in the description of the other subsystem. The coupling between the charge-ordering is characterized by nonzero $\langle T_{ij}^z \rangle$ and $\langle T_{i+1j}^z \rangle$ and the superexchange coupling J_{ij} along the ladder is negative. With increasing charge ordering along a ladder the effective superexchange coupling J_{ij} decreases as shown in Fig. 4. This may change, though, if we include the effect of lattice distortions accompanying the charge ordering. We then have to deal with a combination of effects on J_{ij} as argued above.

We first consider Eq. (11) for each of the two subsystems separately and then discuss the combined ordered ground state. We can make a Wigner-Jordan transformation of the spin operators of a subsystem to obtain spinless fermions describing the spin degrees of freedom. Let $k_F = \pi/2b$ be the Fermi momentum of these spinless fermions where b is the lattice constant in the b direction.

For a single subsystem, e.g., subsystem 1, alternation of the superexchange J_{ij} along the Heisenberg chains can be obtained by shifting the Na ions alternatingly in the c direction or by shifting the O ions on the rungs in the b direction as shown in Fig. 5. Applying the result of Cross and Fisher[40] we arrive at renormalized phonon frequencies for $q = 2k_F$:

$$\tilde{\omega}_{2k_F,O_R}^2 = \omega_{2k_F,O_R}^2 - 0.26|2g_{O_R}(2k_F)|^2 T^{-1},$$

$$\tilde{\omega}_{2k_F,Na}^2 = \omega_{2k_F,Na}^2 - 0.26|g_{Na}(2k_F)|^2 T^{-1}. \qquad (14)$$

The coupling of a shift of the Na ion to a superexchange alternation is smaller by a factor of 2, because a shift of the Na site in the c direction affects the superexchange only on one two-rung cluster whereas a shift of the rung O site in the b direction affects the superexchange on two neighboring two-rung clusters.

For a single subsystem, e.g., subsystem 1, there is also an instability towards superexchange alternation along the
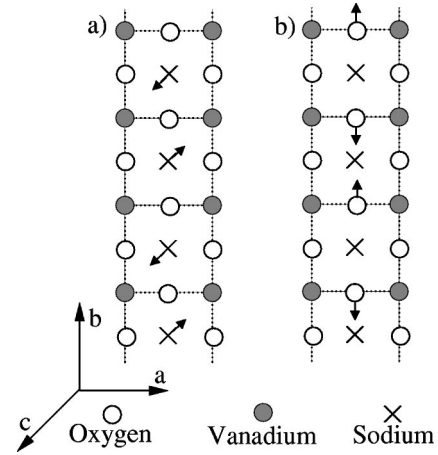

FIG. 5. (a) Alternating Na shift in the c direction schematically shown by arrows causes superexchange alternation. (b) Alternating shift of the rung O ions in the b direction causing superexchange alternation and inequivalence of the Na sites along the ladder.

Heisenberg chains accompanied by charge ordering along the Ising chains. This corresponds to shifts induced by the lattice mode q_0 with $q_0 = 2k_F$ as shown in Fig. 3. Within this mode the V sites on the chains of the A ladder shift in c direction. The direction of the shift alternates along the ladder, corresponding to a staggered longitudinal field for the pseudospins of subsystem 1. The leg O ions on the B ladders also shift in the c direction together with the neighboring V sites of the A ladder. This causes an alternation of the superexchange along the B ladder, corresponding to an alternation of J_{ij} along the Heisenberg spin chains of subsystem 1. Applying the results of Cross and Fisher and using RPA for the effect of the pseudospin-lattice coupling one obtains

$$\tilde{\omega}_{q_0}^2 = \omega_{q_0}^2 - 0.26|g_{VO}(q_0)|^2 T^{-1} - 4g_{Is}^2 \chi_{q_0}(T), \qquad (15)$$

where the last term describes the influence of the Ising chains. Here $\chi_q(T)$ is the susceptibility of the Ising chain due to a longitudinal field along the z direction. g_{VO} describes the coupling of a shift of the V sites on the superexchange of the neighboring ladder via a shift of the O site.

B. The phase transition at T_{C1}

We know from experiment that the phase transition at T_{C1} in α'-NaV$_2$O$_5$ is accompanied by charge ordering.[5] We therefore first consider Eq. (15). We can take g for the q_0 mode in Fig. 3 directly from the results in[19]

$$g_{q_0}^{VO} = \sqrt{\frac{\hbar}{m_V}} \frac{\delta_J^{exp} J}{d_V} = 7.884 \times 10^9 \ \text{K s}^{-1/2} \qquad (16)$$

with $d_V = 6.0768$ pm being the square root of the average of the squared shifts of the V sites on the A ladder, $\delta_J^{exp} = 0.26$ the exchange dimerization along the B ladders for layer a, $J = 522$ K, and m_V the V ion mass. The large exchange dimerization δ_J^{exp} has been obtained in Ref. 19 from a Slater-Koster-approximation for the distorted phase: It is mostly due to the shift of the oxygen atoms along the leg of the B

ladders. We also need to obtain $\chi_q(T)$. While this is very difficult for general values of q, it is facilitated considerably when $q=q_0$. In this case the effective field for the pseudospins due to the lattice distortion is staggered in the b direction. The Ising chain has an antiferromagnetic coupling $K_{Lz}>0$ along the b direction. Calculating $\chi_{q_0}(T)$ means therefore to calculate the susceptibility of an antiferromagnetic Ising chain in a transverse field for the application of an infinitesimal staggered longitudinal field. This is equivalent to calculating the susceptibility of a ferromagnetic Ising model in a transverse field for the application of an infinitesimal constant longitudinal field. This susceptibility can be expressed via the pseudospin correlation function $\rho(\lambda, T)$

$$\chi_{q_0}(T)=\beta \lim_{N\to\infty}\frac{1}{N}\sum_{i,j=1}^{N}\rho_{|i-j|}^{z}(\lambda,T), \qquad (17)$$

where $\rho_{|i-j|}^{z}(\lambda,T)=\langle T_i^z T_j^z\rangle(\lambda,T)$ and $\beta=1/k_BT$ is the inverse temperature. $\lambda=\widetilde{K}_{Lz}/4\widetilde{t}_R$ is the ratio between the pseudospin interaction and the transverse field and determines the properties of the Ising chain. $\lambda=\infty$ corresponds to the Ising chain without a transverse field, $\lambda=0$ to the paramagnetic limit.

For an Ising chain in a transverse field $\rho_n^z(\lambda,T)$ can be written in the form of a Toeplitz determinant.[34] For large n acccording to Szegö's theorem[41] we have

$$\rho_n^z(\lambda,T)=\frac{1}{4}P(\lambda,T)G^n(\lambda,T), \qquad (18)$$

where expressions for $P(\lambda,T)$ and $G(\lambda,T)$ are found in Ref. 42. Some simple limits are given below. To obtain $\chi_{q_0}(T)$ we assume that the asymptotic expression (18) is correct for all n. With this assumption summation of the series (17) yields

$$\chi_{q_0,\lambda}=\frac{1}{4}\beta P(\lambda,T)\frac{1+G(\lambda,T)}{1-G(\lambda,T)}. \qquad (19)$$

The approximation is expected to be correct close to the quantum critical point, i.e., close to $\lambda=1$ at $T=0$, since then the susceptibility and the correlation length diverge. However, we can obtain $P(\lambda,T)$ and $G(\lambda,T)$ for the case $\lambda=\infty$, i.e., the pure Ising chain, from Ref.[42] as

$$P_{\lambda=\infty}=1,$$

$$G_{\lambda=\infty}=\tanh(\beta\widetilde{t}_R\lambda). \qquad (20)$$

When $\lambda=0$ we are in the paramagnetic regime and find

$$P_{\lambda=0}=\frac{2}{2\beta\widetilde{t}_R}(1-\lambda^2)^{-3/4}=\frac{2}{2\beta\widetilde{t}_R},$$

$$G_{\lambda=0}=\lambda\{\tanh[\beta\widetilde{t}_R(1+\lambda)]\}\exp\{(2\pi\beta\widetilde{t}_R)^{-1/2}$$

$$\times\exp[-\beta\widetilde{t}_R(1-\lambda)]\cdots\}=0. \qquad (21)$$

With these expressions we can calculate $\chi_{q_0}(T)$ in the limits $\lambda=\infty$, 0 and find

$$\chi_{q_0,\lambda=\infty}(T)=\frac{\beta}{4}\exp\left(\frac{1}{2}\beta\widetilde{K}_{Lz}\right) \qquad (22)$$

and

$$\chi_{q_0,\lambda=0}(T)=\frac{1}{2(2\widetilde{t}_R)}\tanh\left(\frac{1}{2}\beta(2\widetilde{t}_R)\right). \qquad (23)$$

Both expressions (22) and (23) are equal to the exact solution in these limits which implies that this $\chi_{q_0,\lambda}$ should be a reasonable approximation for all values of λ. We can therefore in principle calculate T_{C1} from Eq. (15) knowing g_{Is}, ω_{q_0}, and λ by simply setting $\widetilde{\omega}_{q_0}=0$.

We can find ω_{q_0} from measurements of the elastic constants.[43] There a strong anomaly in the c_{66} mode of α'-NaV$_2$O$_5$ was observed at the phase transition temperature. This mode couples to a zig-zag-like charge ordering and we therefore identify it with the q_0 mode of the present calculations. Using the high-temperature value for the sound velocity $v_{66}=4200$ m/s we estimate $\omega_{q_0}=\pi v_{66}/b=279$ K, where $b=3.611$ Å is the lattice constant in the b direction for the undistorted lattice.

When ω_{q_0} is known we obtain λ and g_{Is} by fitting them to $T_{C1}=34$ K and to the experimental value of the shift of T_{C1} in a magnetic field. The latter is reduced from its standard spin-Peierls value[44] due to the Ising part of the transition. This is seen as follows. Considering only the spin-Peierls part of the transition, applying a magnetic field lowers the transition temperature $T_{C1}(H=0)$ without a magnetic field to a value $T_{C1}^{H,SP}$. On the other hand, the Ising chain susceptibility $\chi_{q_0,\lambda}(T)$ increases with decreasing temperature. This causes an increase of the critical temperature from $T_{C1}^{H,SP}$ to the observed phase transition temperature $T_{C1}(H)>T_{C1}^{H,SP}$ in a magnetic field.

The expansion for T_{C1} in a magnetic field H for a pure spin-Peierls system is[44]

$$\frac{T_{C1}(H)-T_{C1}(H=0)}{T_{C1}(H=0)}=-0.36\left(\frac{\mu_B H}{k_B T_{C1}(H=0)}\right)^2. \qquad (24)$$

Due to the influence of the Ising part this expression is modified to

$$\frac{T_{C1}(H)-T_{C1}^H}{T_{C1}^{H,Is}(0)}=-0.36\left(\frac{\mu_B H}{k_B T_{C1}^{H,Is}(0)}\right)^2$$

$$\frac{k_B T_{C1}^{H,Is}}{J}(0)=0.8\frac{(g_{q_0}^{VO})^2}{\pi J\omega_{q_0,\mathrm{eff}}^2[T_{C1}(H)]} \qquad (25)$$

in the present case with

$$\omega_{q_0,\mathrm{eff}}^2[T_{C1}(H)]=\omega_{q_0}^2-4g_{Is}^2\chi_{q_0,\lambda}[T_{C1}(H)]. \qquad (26)$$

For small shifts this leads to

$$\frac{T_{C1}(H)-T_{C1}(0)}{T_{C1}(0)}=-\frac{0.36}{1+T_{C1}(0)a[T_{C1}(0)]}\left(\frac{\mu_B H}{k_B T_{C1}(0)}\right)^2$$
$$(27)$$

with

$$a(T)=-\frac{4g_{Is}^2[d\chi_{q_0,\lambda}(T)/dT]}{\omega_{q_0}^2-4g_{Is}^2\chi_{q_0,\lambda}(T)}. \qquad (28)$$

From the experimental result for the shift of $T_{C1}=34$ K in a magnetic field in Refs. 4,25,24 we obtain $a(T_{C1})\approx 0.086$ K^{-1}. Fitting g_{Is} and λ to these two values we obtain

$$\lambda=0.99850,$$

$$g_{Is}=1.688 \ \ \text{K/(pm shift of V).} \qquad (29)$$

Note that this value for λ is close to the value for the ratio $K_{IL}/K_{Lz}\approx 0.997$ from Eq. (9). This indicates that geometrical frustration plays an important role. To see how stable the solution is towards a change of the parameters, we evaluate the dependence of T_{C1} on $\widetilde{K}_{Lz}$, ω_{q_0}, and g_{Is}:

$$\frac{\partial T_{C1}}{\partial \widetilde{K}_{Lz}}=1.06,$$

$$\frac{\partial T_{C1}}{\partial \omega_{q_0}}=-0.14,$$

$$\frac{\partial T_{C1}}{\partial g_{Is}}=12 \ \ \text{pm.} \qquad (30)$$

T_{C1} is rather sensitive to small changes of $\widetilde{K}_{Lz}$ or λ. This sensitivity is due to the fact, that $(1-\lambda)\ll 1$. It is much less and the stability therefore much improved compared to the result presented in Ref. 29, where $\lambda\approx 0.99986$ was suggested.

Next we include the coupling between the two subsystems. For this we will use the mean-field values for $\langle T_{ij}^z\rangle,\langle T_{i+1j}^z\rangle$. They are zero at T_{C1} and therefore the critical temperature T_{C1} remains unchanged in this approximation. But a mean-field approximation is not reliable close to the critical point of the transition where fluctuations must be taken into account. We therefore consider the zero temperature free energy of different ordered states. For this we need the dependence of the superexchange J_0^{ij} along a ladder on the charge ordering order parameter $\langle T_j^z\rangle$ on the same ladder. This is approximately

$$J_{ij}^{\text{eff}}=J_0^{ij}(1-4\langle T_j^z\rangle^2), \qquad (31)$$

where we neglect a small contribution to J_{ij}^{eff} from the diagonal hopping in the case of complete charge ordering on the ladder, i.e., for $\langle T_j^z\rangle=\frac{1}{2}$. As argued at the end of Sec. II, J_{ij}^{eff} enters our equations in two places. First, it effectively changes ω_{q_0} through $J_0 f(T_{ij}^z,T_{i+1j}^z)$. Since we used ω_{q_0} from experiment, this effect is already included. Second, J_{ij}^{eff}
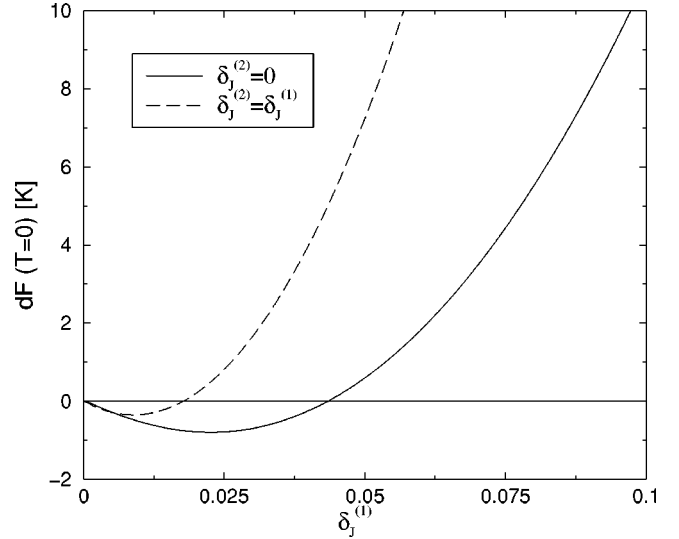

FIG. 6. Ground-state energy gain dF of the ordered system versus the disordered system depending on the order parameters.

modifies the energy gain resulting from the spin degrees of freedom due to distortions and it is this effect we have to consider now. Using the expression for the magnetic energy gain from Ref. 12 for the alternating Heisenberg chain we can write down the energy gain $dF(T=0)$ of the ground-state of the ordered system versus that of the ground-state of the disordered system. The dimerization parameter of the Heisenberg chains $\delta_J^{(1),(2)}$ with $\delta_J^{(1),(2)}=g_{q_0}^{\text{VO}}Q_{1,2}/J$ from Eq. (16) is the order parameter for each of the two subsystems. $Q=d_V\sqrt{m_V/\hbar}$ is the canonical displacement. We find

$$dF(T=0)=b(Q_1^2+Q_2^2)-E_{SP}(Q_1)(1-4\langle T_2^z\rangle^2)-E_{SP}(Q_2)$$
$$\times(1-4\langle T_1^z\rangle^2)-2g_{Is}(\langle T_1^z\rangle Q_1+\langle T_2^z\rangle Q_2) \qquad (32)$$

with

$$b=\frac{1}{2}\omega_{q_0}^2,$$

$$E_{SP}(Q_{1,2})=0.3134J(\delta_J^{(1),(2)})^{4/3},$$

$$\langle T_{1,2}^z\rangle=\frac{1}{2}\{1-\exp[-4\chi_{Is}(T=0)g_{Is}Q_{1,2}]\}. \qquad (33)$$

Here we assumed that T^z approaches $\frac{1}{2}$ exponentially if a staggered parallel field $g_{Is}Q$ is applied. In Eq. (32) E_{SP} denotes the energy gain from the spin-Peierls distortions, while the terms proportional to g_{Is} denote the energy gain from charge ordering. The first term stands for the elastic energy of the distortion. Optimizing Eq. (32) in $\delta_J^{(1),(2)}\in[0,1]$ we find a minimum at $\delta_J^{(1)}=0.023$, $\delta_Q^{(2)}=0$ or vice versa with $dF=-0.80$ K. Requiring $\delta_J^{(1)}=\delta_J^{(2)}=\delta_J$, i.e., the equivalence of the two subsystems we find $\delta_J=0.009$ with $dF=-0.35$ K. We have plotted in Fig. 6 dF for $\delta_J^{(1)}=\delta_J^{(2)}$ and $\delta_J^{(2)}=0$. In the previous calculations we used

$\delta_J^{\mathrm{exp}}=0.26$ to obtain $g_{q_0}^{\mathrm{VO}}$, so the first result is more consistent with our calculation than the second one and it also has the lower energy.

From the derivation of χ_{Is} we can obtain the bare correlation length along the Ising chains as

$$\xi_{Is}(T)=-\frac{1}{\ln G(T)}. \qquad (34)$$

At T_{C1} we find that $\xi_{Is}\approx 183$ lattice constants. This large value of ξ_{Is} might offer an explanation for the strong dependence of T_{C1} on doping. By substituting Na with Ca or depleting the system of Na additional electrons/holes are introduced into the system. This implies double/zero occupancy of rungs. They weaken correlations along the Ising chains. A rough estimate of the critical doping value at which the phase transition temperature T_{C1} is suppressed is $x_C\approx 0.5\%$. We obtain it by assuming $x_C\xi_{Is}\approx 1$. This value is in qualitative agreement with experiment. Substituting Na by Ca the transition disappears between 1 and 2.5% of Ca.[45] For hole doping due to Na deficiency the transition disappears between 2 and 3% deficiency.[46]

C. The phase transition at T_{C2}

Next we consider the second phase transition observed. According to Ref. 5 this transition is of the Ginzburg-Landau type. It opens a spin gap and creates a local distortion at the Na sites as observed from the changes of the quadrupolar electric field tensor. Charge ordering at the V sites starts before this transition sets in (Ref. 5). For these reasons and in order to explain the observation of eight inequivalent Na sites in ^{23}Na-NMR (Refs. 5,47) we suggested in Ref. 19 that the opening of the spin gap in the system is due to an alternating shift of the Na ions along the charge-ordered A ladders as shown in Fig. 5(a). A second possibility is an alternating shift of the rung O ions on the A ladders as shown in Fig. 5(b).

By using the hopping matrix elements obtained in Ref. 19 for the charge-ordered ladder in layer a we can calculate the effective superexchange J dependence on the charge ordering δ_{CO} on the same ladder. As we did for the undistorted ladders (see Fig. 4), the superexchange is defined by the singlet-triplet gap on a two-rung cluster. It is obtained via exact diagonalization. We know from experiment[2] that $J\approx 440$ K in the low-temperature phase. This value of J corresponds to an incomplete charge ordering $\delta_{\mathrm{CO}}^0=\frac{1}{2}(n_+-n_-)\approx 0.32$ on the A ladders in agreement with experiment.[5]

The hopping matrix elements t_L, t_D, t_R change due to the distortion accompanying the charge ordering.[19] We parametrize these changes with $t(\delta_{\mathrm{CO}}=0)-t(\delta_{\mathrm{CO}})\propto\delta_{lat}\propto\delta_{\mathrm{CO}}$, and normalize the prefactors such that the hopping matrix elements from Ref. 19 for the high temperature undistorted ladder are obtained at $\delta_{\mathrm{CO}}=0$ and those for the charge ordered ladder are obtained at $\delta_{\mathrm{CO}}=\delta_{\mathrm{CO}}^0$.

Due to alternating shifts of the rung O ions or the Na ions, the effective hopping along the leg t_L and the effective diagonal hopping t_D alternate also. The size of this is given by the parameter $\delta_{t_{L,D}}=(t_+^{L,D}-t_-^{L,D})/(t_+^{L,D}+t_-^{L,D})$. If we know
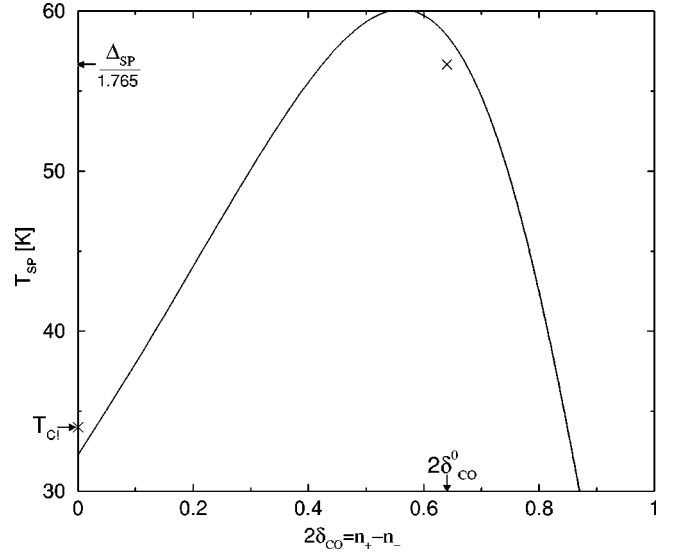

FIG. 7. T_{SP} dependence on charge ordering for a spin-Peierls transition due to alternating shifts of the rung O ions on the A ladders in the b direction. Dimerisation of hopping matrix elements for a shift of 1 pm given by $\delta_{t_D}=0.090$ and $\delta_{t_L}=-0.059$. $\times$ mark conditions (i) and (iii) (see text). The increase of T_{SP} for small δ_{CO} is due to increase of the effective δ_J resulting from increase of the hopping matrix elements due to the distortion accompanying the charge ordering. The decrease for large δ_{CO} is caused by the decrease of the average superexchange $\bar{J}$ as shown in Fig. 4.

δ_{t_L} and δ_{t_D} we can find the superexchange alternation parameter δ_J by calculating the superexchange for the inequivalent two-rung clusters.[19] This gives us an approximate value for the spin-lattice coupling. Using it, the parametrized t_L, t_D, and t_R from above, and Eq. (14) for the critical temperature we find $T_{\mathrm{SP}}(\delta_{\mathrm{CO}})$ for a spin-Peierls transition depending on the charge ordering:

$$\frac{k_B T_{\mathrm{SP}}(\delta_{\mathrm{CO}})}{J(\delta_{\mathrm{CO}})}=0.8\frac{4g_{\mathrm{O}x}^2(\delta_{\mathrm{CO}})}{\pi J(\delta_{\mathrm{CO}})\omega_{\mathrm{O}x}^2}. \qquad (35)$$

We can estimate the value $\omega_{\mathrm{O}x}$ from the velocity v_{22} of the c_{22} mode in Ref. 43. It describes a longitudinal mode along the b direction as required for the proposed shifts of the rung O ions with $v_{22}=6500$ m/s which yields $\omega_{\mathrm{O}x}=432$ K. For given values of δ_{t_L} and δ_{t_D} we obtain the dependence of the critical temperature T_{SP} on the charge ordering δ_{CO} as shown in Fig. 7. In the low-temperature limit the spin gap is approximately given by $\Delta(\delta_{\mathrm{CO}}^0)\approx 1.8 T_{\mathrm{SP}}(\delta_{\mathrm{CO}}^0)$. Therefore the BCS ratio is enhanced by a factor of $T_{\mathrm{SP}}(\delta_{\mathrm{CO}}^0)/T_{C1}$.

We search for values of δ_{t_L} and δ_{t_D} for which the following conditions are fulfilled. (i) Without charge ordering the critical temperature for such a transition is below 34 K, since the spin gap opens only below the charge ordering temperature. (ii) With increasing charge ordering the critical temperature is required to increase, because an enhanced BCS ratio has been observed. (iii) At $\delta_{\mathrm{CO}}=\delta_{\mathrm{CO}}^0$ the spin gap $\Delta(\delta_{\mathrm{CO}})\approx 1.8 T_C^{\mathrm{SP}}(\delta_{\mathrm{CO}}^0)$ should be approximately 100 K as found experimentally.

TABLE I. Change of hopping matrix elements for an alternating Na shift in the c direction, an alternating V shift in the b direction, and an alternating shift of rung O ions in the b direction, respectively. Shift is by 1 pm per site on an otherwise undistorted ladder. The accompanying change of the superexchange has been calculated as the singlet-triplet gap on a cluster of two neighboring rungs of a ladder (Ref. 19).

	$\delta_{t_D} = \dfrac{t_{D+} - t_{D-}}{t_{D+} + t_{D-}}$	δ_{t_L}	$\delta_J = \dfrac{J_+ - J_-}{J_+ + J_+}$
Na shift in the c the direction	0.0105	−0.0135	0.0035
V shift in the b the direction	0.0236	0.0136	0.0347
Rung O shift in the b direction	0.0072	−0.0093	−0.0016
Rung O shift in the b direction with t_{OO} included	0.102	0.003	0.096

The result is found in Fig. 7. The conditions (i)–(iii) are fulfilled for $\delta_{t_L} = -0.059$, $\delta_{t_D} = 0.090$, and with $T_{C1} = 34$ K an effective BCS ratio of 6.05 is found. We therefore have a spin-Peierls phase transition which is driven by charge ordering on the same ladder. When the first transition takes place at about $T_{C1} = 34$ K charge ordering sets in on the A ladders. This changes the two-particle correlation functions and the effective hoppings so that T_{SP} increases as compared with its value without charge ordering. At some temperature $T_{C2} < T_{C1}$ we have $T_{SP}[\delta_{CO}(T_{C2})] = T_{C2}$ and a spin-Peierls transition driven by charge ordering takes place. This is caused by an alternating shift of the O ions on the rungs of the A ladders, probably together with a small alternating shift of the Na ions along the A ladders. This also causes an inequivalence of the Na sites along the A ladders, such that we have eight inequivalent Na sites as observed in experiment.[47] Since this happens before δ_{CO} attains its final value, the spin gap at lower temperatures is larger than what would be expected from the standard BCS ratio and T_{C1}.

In order to see whether the values for δ_{t_L} and δ_{t_D} are plausible, we have investigated the effects of alternating shifts of the rung O or the Na sites on the effective hopping matrix elements between V sites on the ladders. For this we use the Slater-Koster method as described in Ref. 19. The results are given in Table I. Those for δ_{t_L} and δ_{t_D} have been obtained for otherwise undistorted ladders. δ_{t_L} and δ_{t_D} are found to have opposite signs, as assumed above. This can be understood by noticing that an increase of diagonal hopping due to increased hopping via the Na sites goes together with a decrease of the hopping along the legs of the ladder. The effects of charge ordering distortions and of the shifts of Na or rung O sites on the hopping matrix elements are small. Therefore we may neglect higher-order effects resulting from combinations of the distortions.

The results in the first three rows of Table I are based on Ref. 19, where we included V-O, V-V, and Na-O hopping matrix elements in the initial Hamiltonian, projecting these

on effective V-V hopping matrix elements. However, it has been argued in Ref. 30 that direct hopping between the O sites should also contribute to the effective Hamiltonian. It remains unclear which fraction of the total O-O hopping matrix elements obtained in Ref. 30 results from direct hopping and which fraction comes from indirect hopping via the neighboring Na site. To investigate the effect of such a hopping on the shifts of the rung O ions we introduced O-O hopping matrix elements according to the Slater-Koster approximation for into the initial Hamiltonian and calculated effective V-V hopping matrix elements as before. One finds $t_R = -0.17$ eV, $t_L = 0.17$ eV, $t_D = -0.04$ eV, $t_{IL} = -0.16$ eV. Introducing an alternating shift of the rung O ions in the b direction by 1 pm leads to $\delta_{t_L} \approx 0.003$ and $\delta_{t_D} \approx 0.1$ as given in the fourth row of Table I. The effect especially on the diagonal hopping is much stronger than it is without inclusion of the direct O-O hopping matrix elements. However, these values for t_L and t_{IL} are far from those found by LDA (Ref. 30) and *ab initio* methods.[48] One can therefore conclude that at least within the Slater-Koster method the contribution of the direct O-O hopping should be small as expected for next-nearest-neighbor hopping, although it may help to explain the small differences between the LDA results of Ref. 30 and our results in Ref. 19. The results from Table I can serve only as an estimate of the values of the spin-lattice coupling.

In this section we have investigated how the model Hamiltonian of Eq. (11) leads to two consecutive phase transitions. First at T_{C1} a combined spin-Peierls Ising transition leads to inequivalent exchange dimerized and charge ordered ladders which removes the geometric frustration of the Trellis lattice. The increasing charge order on the A ladders enhances their effective coupling to a dimerization mode connected with the Na shifts which leads then immediately below at T_{C2} to another dimerization transition on the B ladders which opens the spin gap.

IV. COMPARISON WITH X-RAY DIFFRACTION AND NEUTRON SCATTERING EXPERIMENTS

In the following we compare our results with experimental observations. We do this with respect to two types of experiment: x-ray structure determination[17–19] and inelastic neutron scattering results for the magnon dispersion.[2,3] We compute the latter for the calculated structure by using a local-dimer approximation. We do not consider the Raman spectroscopy experiments here, in which a sharp peak at 65 cm^{-1} is observed.[49] This peak might be due to a charge transfer excitation for which the interladder Coulomb repulsion and the resulting two-dimensional character of the excitation play a significant role.

Comparing our results with x-ray structure determination we find good agreement. In both cases we have a superstructure consisting of two inequivalent ladder types alternating along the a direction: charge-ordered A ladders and strongly dimerized B ladders. A phase with two A ladders separated by a B ladder is also correctly found. We can explain these findings with the analysis given in Sec. III B: the displacement of the V sites on the A ladders and of the O sites on the
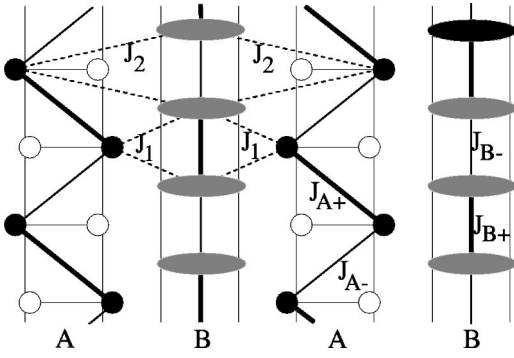
FIG. 8. Geometry of initial magnetic Hamiltonian (36). $J_{\pm}$ $=J(1\pm\delta)$ for the respective ladder.
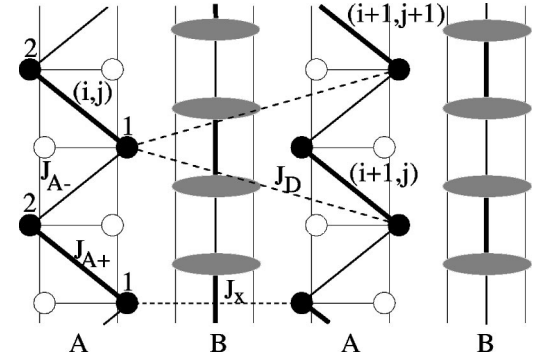

FIG. 9. Geometry of effective magnetic Hamiltonian (37). 1 and 2 denote the two spins of a dimer, J_A and J_D denote the effective superexchange between spins in the A ladder via the B ladder for nearest interladder neighbors and next-nearest interladder neighbors. V_{21} sites with increased electron density denoted by black circles, V_{22} sites with decreased electron density by white circles.

B ladders cause a combined charge-ordering-spin-Peierls transition.

X-ray structure analysis finds $Fmm2$ symmetry in the low-temperature phase. In our model this symmetry is realized for $T_{C1}>T>T_{C2}$. However, the phase transition at T_{C2} obtained for our model in Sec. III C is accompanied by a breaking of this symmetry. It results from the shift of the rung O ions on the A ladders, as shown in Fig. 5(b). A low-temperature spin gap of $\Delta\approx100$ K on these ladders requires a superexchange dimerization of about 0.05 when Δ $=2J\delta_J^{3/4}$ from Ref. 12 is used with the experimental value for $J=440$ K. The coupling constant at $\delta_{CO}^0=0.32$ is approximately 0.043 per pm shift of the rung O ion. This corresponds to an actual shift of 1.1 pm of each rung O ion on ladder A.

The intensity of the x-ray scattering for small scattering angles is proportional to Z^2 where Z is the ionic charge. Below T_{C2} only one O ion per two formula units shifts its position to break the $Fmm2$ symmetry. In addition as estimated above these displacements are smaller than the displacements caused by the phase transition at T_{C1} and below, where a displacement of 7.46 and 4.26 pm for the V sites on the A ladder is found experimentally. It is therefore well possible that the scattering peaks resulting from the lower symmetry cannot be observed within experimental resolution. Insofar x-ray structure determization results do not contradict our theoretical results for the second transition.

Magnon dispersion, however, should be greatly affected by a dimerization. The structure which is obtained after the two transitions have taken place is schematically shown in Fig. 8. The calculated magnon dispersion for this structure should therefore be a good test of the theory. For other suggested structures it was found that the corresponding magnon dispersion disagrees with experimental results: in the case of a lattice with zig-zag charge order on all ladders and assuming identical exchange alternation on all ladders and a possible exchange anisotropy the dispersion along the a direction does not agree with experiments[50]. A theoretical model using charge ordering and different exchange alternation along all ladders has been considered in Ref. 3. For the spin-cluster model proposed in Ref. 18 the magnon dispersions, both in the a and b directions, do not agree with experiments either.[51–53]

We therefore calculate the magnon dispersion at a tem-

perature well below T_{C2}. In order to do this we use the spin-dimer representation following Refs. 50,54,55. The initial magnetic Hamiltonian is then

$$H=\sum_{i\in A}J_A(1+(-1)^j\delta_A)\vec{S}_{ij}\vec{S}_{ij+1}$$

$$+\sum_{i\in B}J_B(1+(-1)^j\delta_B)\vec{S}_{ij}\vec{S}_{ij+1}+\sum_{\langle ij,mn\rangle}J_{IL}^{ij,mn}\vec{S}_{ij}\vec{S}_{mn} \tag{36}$$

for a geometry and $J_{IL}^{ij,mn}$ as shown in Fig. 8. It describes the pure spin part of Eq. (11) with the effects of lattice distortions and pseudospins included within the effective coupling constants. The large value of $\delta_B\approx0.26$ at $T=15$ K found in Ref. 19 corresponds to a large gap in the excitation spectrum of the B ladders. Using $\Delta_B=2J_B\delta_B^{3/4}$ for the spin gap[12] and $J_B=52$ meV from Ref. 19 we find $\Delta_B\approx38$ meV. The B ladders should therefore not contribute directly to the low-lying parts of the magnon dispersion. Since we are only interested in these, we assume that we have an indirect exchange coupling between A ladders through the virtual singlet-triplet excitations of the B ladders. This results in an effective Hamiltonian

$$H=\sum_{ij\gamma}J_A(1+(-1)^j\delta_A)\vec{S}_{ij\gamma}\vec{S}_{ij+1\gamma}+\sum_{ij\gamma}J_a\vec{S}_{ij\gamma}\vec{S}_{i+1j\gamma}$$

$$+\sum_{ij\gamma}J_D\vec{S}_{ij\gamma}(\vec{S}_{i+1j+1\gamma}+\vec{S}_{i+1j-1\gamma})+\sum_{ij\gamma}J_c\vec{S}_{ij\gamma}\vec{S}_{ij\bar{\gamma}} \tag{37}$$

with corresponding geometry and couplings as shown in Fig. 9. This exchange Hamiltonian exhibits manifestly a doubling of the period along the a axis. Here we also introduced a superexchange J_c in the c direction between layers; it is assumed to exist mainly between the V_{21} sites which lie directly above each other.[19] We therefore have $\gamma=\pm1$: Along the c direction the V sites of the A ladder are ordered as $\cdots-V_{21}-V_{21}-V_{22}-V_{22}-\cdots$ as shown in Fig. 10.[17–19] Next
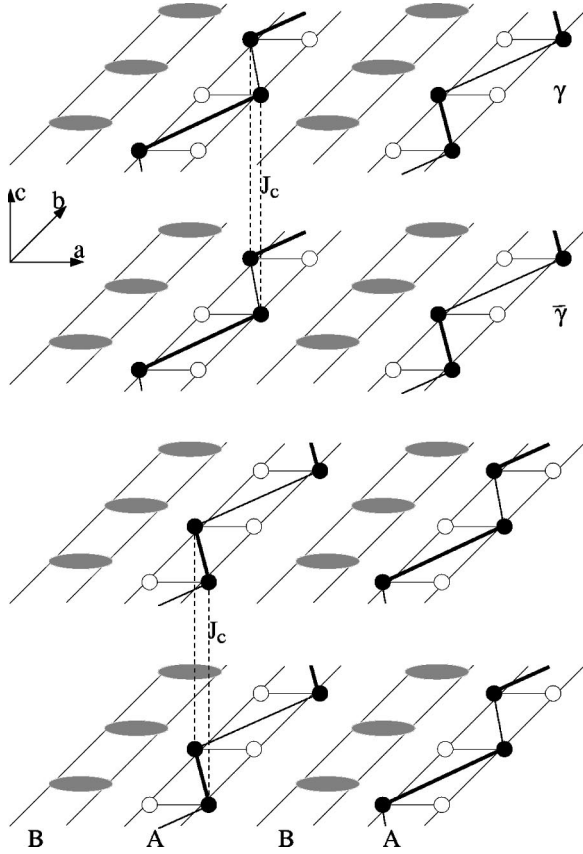
FIG. 10. Unit cell of low-temperature ordered state. Along the A ladders one has pairs of V_{21} sites (black circles) alternating with pairs of V_{22} sites (white circles) in the c direction. J_c therefore connects two layers γ, $\bar{\gamma}$ only. For such two layers, dimers on the A ladders are assumed to lie directly above each other in the c direction.

we introduce dimer variables. We denote each dimer within the A ladder (see Fig. 9) by coordinates $ij\gamma$, which are not identical with the former coordinates of the spins. As denoted in Fig. 9 we then have spins $\vec{S}_{ij\gamma1,2}$. The dimer variables are then

$$\vec{K}_{ij\gamma}=\vec{S}_{ij\gamma1}+\vec{S}_{ij\gamma2},$$

$$\vec{L}_{ij\gamma}=\vec{S}_{ij\gamma1}-\vec{S}_{ij\gamma2}. \tag{38}$$

With those, Eq. (37) takes the form

$$H=\frac{1}{4}J_A(1+\delta_A)\sum_{ij\gamma}\vec{K}_{ij\gamma}\vec{K}_{ij\gamma}-\vec{L}_{ij\gamma}\vec{L}_{ij\gamma}$$

$$+\frac{1}{4}J_A(1-\delta_A)\sum_{ij\gamma}\vec{K}_{ij\gamma}\vec{K}_{ij+1\gamma}-\vec{L}_{ij\gamma}\vec{L}_{ij+1\gamma}$$

$$+\frac{1}{4}J_a\sum_{ij\gamma}\vec{K}_{ij\gamma}\vec{K}_{i+1j\gamma}-\vec{L}_{ij\gamma}\vec{L}_{i+1j\gamma}$$

$$+\frac{1}{4}J_D\sum_{ij\gamma}(\vec{K}_{ij\gamma}-\vec{L}_{ij\gamma})(\vec{K}_{i+1j\gamma}-\vec{L}_{i+1j\gamma}+\vec{K}_{i+1j+1\gamma}$$

$$-\vec{L}_{i+1j+1\gamma})+(\vec{K}_{ij\gamma}+\vec{L}_{ij\gamma})(\vec{K}_{i+1j\gamma}+\vec{L}_{i+1j\gamma}$$

$$+\vec{K}_{i+1j+1\gamma}+\vec{L}_{i+1j+1\gamma})+\frac{1}{2}J_c\sum_{ij\gamma}\vec{K}_{ij\gamma}\vec{K}_{ij\bar{\gamma}}+\vec{L}_{ij\gamma}\vec{L}_{ij\bar{\gamma}}. \tag{39}$$

As in Ref. 50 we will only use the products $L_{ij\gamma}L_{mn\gamma'}$, since the other terms do not contribute to the dispersion of the spin excitations. We then transform the $\vec{L}$ to

$$\vec{L}_{ij\gamma}=\frac{1}{\sqrt{2}}(\vec{M}_{ij}^{+}+\vec{M}_{ij}^{-}),$$

$$\vec{L}_{ij\bar{\gamma}}=\frac{1}{\sqrt{2}}(\vec{M}_{ij}^{+}-\vec{M}_{ij}^{-}). \tag{40}$$

Furthermore we assume that the ladder designated by ($i+1,\gamma$) is equivalent to the ladder ($i,\bar{\gamma}$). This corresponds to a geometry of the A ladders shown in Fig. 10. We therefore set $L_{ij\gamma}=L_{i+1j\bar{\gamma}}$, and separate the Hamiltonian into two parts:

$$H_{M^+}=-\frac{1}{4}[J_A(1+\delta_A)-J_c]\vec{M}_{ij}^{+}\vec{M}_{ij}^{+}$$

$$-\frac{1}{4}J_A(1-\delta_A)\vec{M}_{ij}^{+}\vec{M}_{ij+1}^{+}-\frac{1}{4}J_a\vec{M}_{ij}^{+}\vec{M}_{i+1j}^{+}$$

$$-\frac{1}{2}J_D(\vec{M}_{ij}^{+}\vec{M}_{i+1j}^{+}+\vec{M}_{ij}^{+}\vec{M}_{i+1j+1}^{+}),$$

$$H_{M^-}=-\frac{1}{4}[J_A(1+\delta_A)+J_c]\vec{M}_{ij}^{-}\vec{M}_{ij}^{-}$$

$$-\frac{1}{4}J_A(1-\delta_A)\vec{M}_{ij}^{-}\vec{M}_{ij+1}^{-}+\frac{1}{4}J_a\vec{M}_{ij}^{-}\vec{M}_{i+1j}^{-}$$

$$-\frac{1}{2}J_D(\vec{M}_{ij}^{-}\vec{M}_{i+1j}^{-}+\vec{M}_{ij}^{-}\vec{M}_{i+1j+1}^{-}). \tag{41}$$

The first term of each Hamiltonian describes an effective dimer with interaction strength $J_A(1+\delta_A)\pm J_c$. Its dynamical susceptibility is

$$u_{\alpha\beta}^{\pm}(\omega)=\delta_{\alpha\beta}(\delta_{\alpha x}+\delta_{\alpha y})\frac{2[J_A(1+\delta_A)\mp J_c]}{[J_A(1+\delta_A)\mp J_c]^2-\omega^2}. \tag{42}$$

The dynamical RPA susceptibility of coupled dimers without anisotropy of the superexchange is given by

$$\chi(\vec{q},\omega)=[1-J(\vec{q})u_{xx}(\omega)]^{-1}u_{xx}(\omega), \tag{43}$$

where J is the exchange term between dimers as given by the last four terms of H_{M+} and H_{M-}. After Fourier transformation these, J^+ for H_{M+} and J^- for H_{M-} are given by

$$J^{\pm}(\vec{q}) = \frac{1}{2} J_A (1 - \delta_A) \cos 2k_y$$

$$\pm \left(\frac{1}{2} J_a \cos(k_x - k_y) - 2 J_D \cos k_x \cos k_y \right). \quad (44)$$

Here $k_x = 2\pi q_x / a$, $k_y = 2\pi q_y / b$ with a and b being the lattice constants of the high-temperature unit cell. We note a doubling of the unit cell in the b direction as required before by Eq. (37). The spin-wave excitations are obtained from the poles of $\chi(\vec{q}, \omega)$. With Eqs. (42) and (44) we obtain

$$\omega_{\pm}^2 = [J_A(1 + \delta_A) \mp J_c]^2 - [J_A(1 + \delta_A) \mp J_c]\{J_A(1 - \delta_A)$$

$$\times \cos 2k_y \pm [J_a \cos(k_x - k_y) - 4 J_D \cos k_x \cos k_y]\}.$$

$$(45)$$

We set $J_a^{\text{eff}} = J_a - 4 J_D$ and $J_A = 440$ K, as used in our previous analysis and obtained from experiment.[2] Then we fit the unknown parameters J_a^{eff}, J_c, and δ_A to the experimental values for three of the four gaps obtained from ω_+ and ω_-. These gap values have been observed for $T \leq 4.2$ K at $q_x = 0$, $q_y = \frac{1}{2}$, and $q_x = 0$, $q_y = 1$.[3] Fitting three of the four gaps of sizes 10.9, 10.1, and 9.1 meV we obtain

$$J_a^{\text{eff}} = 0.212 \text{ meV},$$

$$J_c = 0.431 \text{ meV}, \quad (46)$$

$$\delta_A = 0.0310.$$

This determines the fourth gap to be 8.14 meV which is in excellent agreement with the experimental value 8.2 meV from Ref. 3. In the model presented here these spin gaps result from the assumed dimerization of the charge ordered A ladders whereas previously the origin of the spin gaps was suggested to lie in an anisotropy of the superexchange.[50] The dispersion of $\omega^{\pm}$ along the a direction for $q_y = \frac{1}{2}, 1$ is shown in Fig. 11. These curves also agree with experiments.

The low value of J_a^{eff} which causes the dispersion along the a direction is due to an effective coupling of next-nearest-neighbor ladders. Furthermore, J_a is partly compensated due to J_D couplings.

The value for J_c, which causes the gap between the two modes, corresponds to a hopping $t_c \approx 0.021$ eV between neighboring V sites of neighboring layers when $J_c = 4 t_c^2 / U$ and $U = 4$ eV are used. This is in reasonable agreement with the value $t_c = 0.015$ eV found in Ref. 19 from the low-temperature structural data by a Slater-Koster approximation.

We can also obtain the approximate dispersion in the b direction for $q_x = 0$ as shown in Fig. 12. The maximum is at $\omega \approx 55$ meV and agrees nicely with the value $\omega_{\text{max}} = 59.5$ meV estimated in Ref. 2 from experimental data.

In this section we have shown that the results of our analysis in Sec. III agree well with the experimental results of x-ray structure determination. Furthermore we have investigated the dispersion of spin excitations in the ordered state parallel and perpendicular to the chain direction. From comparison with results of inelastic neutron scattering exchange and dimerization parameters have been obtained. We con-
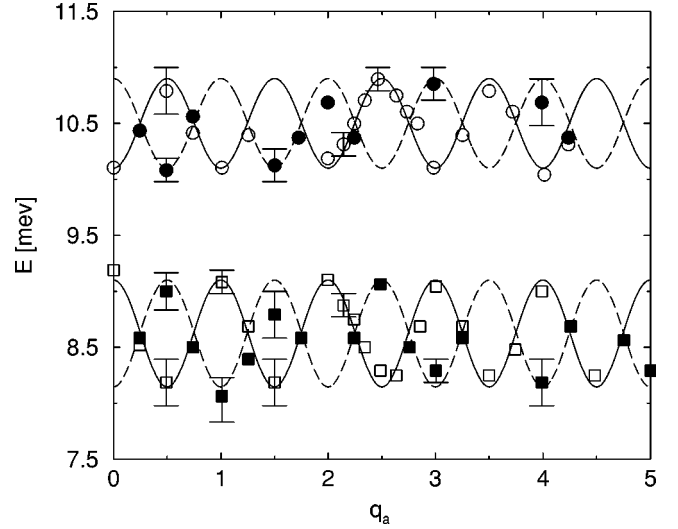

FIG. 11. Magnon dispersion along the a direction for $q_b = \frac{1}{2} = Q_b^{\text{AF}}$ (solid lines) and $q_b = 1 = Q_b^{\text{ZC}}$ (dashed lines). Experimental values from Ref. 3.

clude that the additional zone boundary splitting of spin excitations observed in Ref. 3 is well explained within the inequivalent ladder model.

V. SUMMARY AND CONCLUSIONS

In this article we provided a theoretical description of the phase transitions in α'-NaV$_2$O$_5$. In Sec. II we started from a single band extended Hubbard model describing the hopping of electrons between V sites. We projected this model onto an effective spin-pseudospin Hamiltonian similar to that in Refs. 27–29. Using parameters obtained from a previous Slater-Koster analysis and findings of LDA+U we argued that within the given model a phase transition cannot occur from Coulomb interactions only: the effective lattice for such a transition is triangular and its geometric frustration sup-
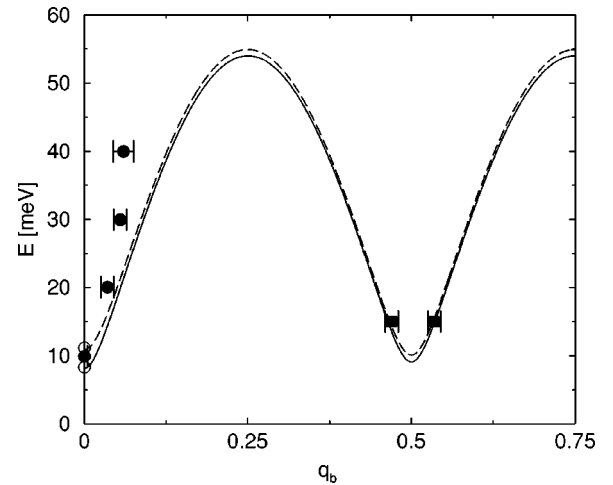

FIG. 12. Magnon dispersion along the b direction for $q_a = 3.5$. Experimental values from Ref. 3 (circles) and Ref. 56 (squares). Above 20 meV the dispersion of the disordered and strongly dimerized B ladders becomes important.

presses charge order, a distinctive feature which is present in the observed transition. We therefore constructed a minimal microscopic model based on a spin-pseudospin Hamiltonian which incorporates the coupling between charges, spins and the lattice.

In Sec. III we analyzed this model with regard to phase transitions. We divided the model into two subsystems. Each of it describes the charge degrees of freedom on the rungs of half the ladders and the spin degrees of freedom on the other ladders. For each subsystem we find an instability towards a transition at T_{C1} which causes "zig-zag" charge ordering and superexchange dimerization. With this combined spin-Peierls-Ising transition we can explain the anomalous shift of T_{C1} in a magnetic field. It is reduced from its normal spin-Peierls value due to the influence of the charge ordering. By calculating the free energy at $T=0$ we found that the system should enter a phase where half of the ladders are "zig-zag" charge-ordered (A ladders), while the other half (B ladders) shows a strong superexchange alternation. The reason for this asymmetry lies in a competition between the order parameters for charge ordering and superexchange dimerization due to a shift of the leg O sites on the same ladder. This explains observations of x-ray structure determination. Due to the strong effect of the one-dimensional Ising chains we can also explain qualitatively the strong dependence of the transition on depletion of Na or substitution of Na with Ca.

By analyzing the coupling between superexchange dimerization and lattice distortion in the charge-ordered ladders we found that another transition is induced. Charge ordering increases the coupling between an alternating shift of the O sites on a rung and the superexchange alternation beyond the threshold value of a second transition at T_{C2}. The system then enters a phase where the charge-ordered A ladders dimerize and a spin gap opens. Due to the alternation the Na sites along the A ladders become inequivalent, such that we have eight inequivalent Na sites as observed in ^{23}Na-NMR,[5,47] not only six as would be the case in the $Fmm2$ symmetry indicated by x-ray structure determination.

This also helps to explain the discrepancy between measurements of the critical exponent of the lattice distortion[9–11] and of the critical exponent of the spin gap opening:[8] the former is smaller than the latter whereas one would expect the opposite for a single transition due to $\Delta \propto \delta_{lat}^{3/4}$. From the observations of a logarithmic peak in the specific heat at T_{C1} and the observation of fluctuations by x-ray diffuse scattering[11] we conclude that the transition at T_{C1} is mainly of 2D Ising character whereas the second transition at T_{C2}, which opens the spin gap, can be described within a mean-field theory. Since the charge ordering is not complete, when the second phase transition is triggered, the coupling constant further increases for decreasing temperatures. This leads to an additional increase of the spin gap and also of the BCS ratio. The conventional BCS ratio does not account for the temperature dependence of the coupling constant $g_{q_0}^{\mathrm{vo}}$.

Within experimental resolution we find agreement with the x-ray structure determination. The second transition breaking the $Fmm2$ symmetry comprises only a small shift of every tenth O site. We also find excellent agreement with experimental results for the magnon dispersion at a temperature well below T_{C2}.

In conclusion we presented a microscopic model for α'-NaV$_2$O$_5$ which yields two phase transitions close to each other. The first is a "spin-Peierls-Ising" transition causing charge order and superexchange dimerization. The second is a pure spin-Peierls transition triggered by an increase of the coupling constant due to charge ordering. With this model we can explain qualitatively and quantitatively a number of experimental observations, i.e., the existence of two transitions, the general structure of the low-temperature phase, the anomalous shift of T_{C1} in a magnetic field, the anomalous BCS ratio, the strong dependence of the transition on doping, and the observed low-energy magnon dispersion.

[1] M. Isobe and Y. Ueda, J. Phys. Soc. Jpn. **65**, 1178 (1996).

[2] T. Yosihama, M. Nishi, K. Nakajima, K. Kakurai, Y. Fujii, M. Isobe, C. Kagami, and Y. Ueda, J. Phys. Soc. Jpn. **67**, 744 (1998).

[3] B. Grenier, O. Cepas, L.P. Regnault, J.E. Lorenzo, T. Ziman, J.P. Boucher, A. Hiess, T. Chatterji, J. Jegoudez, and A. Revcolevschi, Phys. Rev. Lett. **86**, 5966 (2001).

[4] M. Köppen, D. Pankert, R. Hauptmann, M. Lang, M. Weiden, C. Geibel, and F. Steglich, Phys. Rev. B **57**, 8466 (1998).

[5] Y. Fagot-Revurat, M. Mehring, and R.K. Kremer, Phys. Rev. Lett. **84**, 4176 (2000).

[6] D.K. Powell, J.W. Brill, Z. Zeng, and M. Greenblatt, Phys. Rev. B **58**, R2937 (1998).

[7] M. Dischner (private communication).

[8] P. Fertey, M. Poirier, M. Castonguay, J. Jegoudez, and A. Revcolevschi, Phys. Rev. B **57**, 13 698 (1998).

[9] S. Ravy, J. Jegoudez, and A. Revcolevschi, Phys. Rev. B **59**, R681 (1999).

[10] H. Nakao, K. Ohwada, N. Takesue, Y. Fujii, M. Isobe, and Y. Ueda, J. Phys. Chem. Solids **60**, 1101 (1999).

[11] B.D. Gaulin, M.D. Lumsden, R.K. Kremer, M.A. Lumsden, and H. Dabkowska, Phys. Rev. Lett. **84**, 3446 (2000).

[12] T. Barnes, J. Riera, and D.A. Tennant, Phys. Rev. B **59**, 11 384 (1999).

[13] H.G. von Schnering, Y. Grin, M. Kaupp, M. Somer, R.K. Kremer, O. Jepsen, T. Chatterji, and M. Weiden, Z. Kristallogr. - New Cryst. Struct. **213**, 246 (1998).

[14] A. Meetsma, J.L. de Boer, A. Damascelli, J. Jegoudez, A. Revcolevschi, and T.T.M. Palstra, Acta Crystallogr., Sect. C: Cryst. Struct. Commun. **54**, 1558 (1998).

[15] H. Smolinski, C. Gros, W. Weber, U. Peuchert, G. Roth, M. Weiden, and C. Geibel, Phys. Rev. Lett. **80**, 5164 (1998).

[16] T. Ohama, H. Yasuoka, M. Isobe, and Y. Ueda, Phys. Rev. B **59**, 3299 (1999).

[17] J. Lüdecke, A. Jobst, S. van Smaalen, E. Morré, C. Geibel, and H.G. Krane, Phys. Rev. Lett. **82**, 3633 (1999).

[18] J.L. de Boer, SA. Meetsma, J. Baas, and T.T.M. Palstra, Phys. Rev. Lett. **84**, 3962 (2000).

[19] A. Bernert, T. Chatterji, P. Thalmeier, and P. Fulde, Eur. Phys. J. B **21**, 535 (2001).

[20] R. Michalak, H. Mohammad, M. Dischner, and C. Geibel, Physica B **312−313**, 624 (2002).

[21] S. Grenier, A. Toader, J.E. Lorenzo, Y. Joly, B. Grenier, S. Ravy, L.P. Regnault, H. Renevier, J.Y. Henry, J. Jegoudez, and A. Revcolevschi, cond-mat/0109091 (unpublished).

[22] S. van Smaalen, P. Daniels, L. Palatinus, and R.K. Kremer, cond-mat/0108067 (unpublished).

[23] H. Sawa, E. Ninomiya, T. Ohama, H. Nakao, K. Ohwada, Y. Murakami, Y. Fuji, Y. Noda, M. Isobe, and Y. Ueda, cond-mat/0109164 (unpublished).

[24] W. Schnelle, Y. Grin, and R.K. Kremer, Phys. Rev. B **59**, 73 (1999).

[25] S.G. Bompadre, A.F. Hebard, V.N. Kotov, D. Hall, G. Maris, J. Baas, and T.T.M. Palstra, Phys. Rev. B . **61**, R13 321 (2000).

[26] L.N. Bulaewskii, A.I. Buzdin, and D.I. Khomskii, Solid State Commun. **27**, 5 (1978).

[27] P. Thalmeier and P. Fulde, Europhys. Lett. **44**, 242 (1998).

[28] D. Sa and C. Gros, Eur. Phys. J. B **18**, 421 (2000).

[29] M.V. Mostovoy, J. Knoester, and D.I. Khomskii, cond-mat/0009464 (unpublished).

[30] A.N. Yaresko, V.N. Antonov, H. Eschrig, P. Thalmeier, and P. Fulde, Phys. Rev. B **62**, 15 538 (2000).

[31] K. Ohwada, Y. Fujii, N. Takesue, M. Isobe, Y. Ueda, H. Nakao, Y. Wakabayashi, Y. Murakami, K. Ito, Y. Amemiya, H. Fujihisa, K. Aoki, T. Shobu, Y. Noda, and N. Ikeda, Phys. Rev. Lett. **87**, 086402 (2001).

[32] P. Horsch and F. Mack, Eur. Phys. J. B **5**, 367 (1998).

[33] A.B. Harris and R.V. Lange, Phys. Rev. **157**, 295 (1967).

[34] P. Pfeuty, Ann. Phys. (N.Y.) **57**, 79 (1970).

[35] R.M.F. Houtappel, Physica (Amsterdam) **XVI**, 425 (1950).

[36] J. Stephenson, J. Math. Phys. **11**, 420 (1970).

[37] A. Langari, M.A. Martín-Delgado, and P. Thalmeier, Phys. Rev. B **63**, 144420 (2001).

[38] E.Y. Sherman, M. Fischer, P. van Lemmens, P.H.M. Loosdrecht, and G. Güntherodt, Europhys. Lett. **48**, 648 (1999).

[39] V. Yushankhai and P. Thalmeier, Phys. Rev. B **63**, 064402 (2001).

[40] M.C. Cross and D.S. Fisher, Phys. Rev. B **19**, 402 (1979).

[41] U. Grenander and G. Szegö, *Toeplitz Forms and their Applications* (University of California Press, Berkeley, 1958).

[42] B. McCoy, Phys. Rev. **173**, 531 (1968).

[43] H. Schwenk, S. Zherlitsyn, B. Lüthi, E. Morre, and C. Geibel, Phys. Rev. B **60**, 9194 (1999).

[44] M.C. Cross, Phys. Rev. B **20**, 4606 (1979).

[45] M. Dischner, C. Geibel, E. Morré, and G. Sparn, J. Magn. Magn. Mater. **226−230**, 405 (2001).

[46] M. Isobe and Y. Ueda, J. Alloys Compd. **262−263**, 180 (1997).

[47] T. Ohama, A. Goto, T. Shimizu, E.N.H. Sawa, M. Isobe, and Y. Ueda, J. Phys. Soc. Jpn. **69**, 2751 (2000).

[48] N. Suaud and M.B. Lepetit, Phys. Rev. B **62**, 402 (2000).

[49] M.J. Konstantinović, K. Ladavac, A. Belić, Z.V. Popović, A.N. Vasil'ev, M. Isobe, and Y. Ueda, J. Phys.: Condens. Matter **11**, 2103 (1999).

[50] P. Thalmeier and A.N. Yaresko, Eur. Phys. J. B **14**, 495 (2000).

[51] S. Trebst and A. Sengupta, Phys. Rev. B **62**, R14 613 (2000).

[52] A. Honecker and W. Brenig, Phys. Rev. B **63**, 144416 (2000).

[53] C. Gros, R. Valentí, J.V. Alvarez, K. Hamacher, and W. Wenzel, Phys. Rev. B **62**, R14 617 (2000).

[54] B. Leuenberger, A. Stebler, H. U. Güdel, A. Furrer, R. Feile, and J.K. Kjems, Phys. Rev. B **30**, 6300 (1984).

[55] S.B. Haley and P. Erdös, Phys. Rev. B **5**, 1106 (1972).

[56] T. Yosihama, M. Nishi, K. Nakajima, N. Aso, K. Kakurai, Y. Fuji, S. Itoh, C.D. Frost, S.M. Bennington, M. Isobe, and Y. Ueda, Physica B **282&282**, 654 (2000).